X-Disciplinarity

DOI: https://doi.org/10.63174/xdi.LWSA9225

Original Article

Preparation and Mechanism Study of Biochar based Mortar Composite Materials

https://doi.org/10.63174/xdi.LWSA9225

Received: 20 Jul 2025

Accepted: 13 Nov 2025

Published: 16 Nov 2025

Open Access

Ning Song [1, *] Guangqi Hu [2]

Abstract: This study investigated the mechanical properties and hydration mechanism of cement-based composites incorporating rice husk biochar (RB) and corn straw biochar (CB) under standard curing conditions of 28 days. The compressive strength, flexural strength, and total calcium hydroxide generated during hydration of the cement-based composites were studied using simultaneous thermal analysis (TG-DTG), X-ray diffraction (XRD), mercury intrusion porosimetry (MIP), scanning electron microscopy-energy dispersive spectroscopy (SEM-EDS), and attenuated total reflectance Fourier transform infrared spectroscopy (ATR-FTIR). The results showed that when the incorporation of RB and CB was 4%, both the compressive and flexural strengths were significantly improved. The incorporation of RB and CB did not generate new hydration products or change the total amount of calcium hydroxide generated during hydration. On the contrary, refining the internal pore structure of the cement significantly improved the mechanical properties of the cement-based materials. These findings indicate that biochar materials prepared from agricultural and forestry waste represent a valuable new development strategy for improving the performance of cement-based materials.

1. Introduction

Auxiliary cementitious materials are widely used to reduce cement usage and improve the durability of cement-based composite materials. These admixtures mainly use materials such as silica fume to improve the early and long-term strength and durability of cement-based building materials. However, the disadvantage is that they are relatively expensive compared to cement-based materials themselves. In recent years, biochar materials have shown excellent adsorption performance due to their advantages such as large specific surface area and high porosity. Therefore, biochar materials have been widely used in the adsorption of wastewater and soil pollutants[1]. At present, research on the combination of biochar materials and other materials in related fields mainly focuses on carbon dioxide sequestration[2], soil improvement[3-4], water purification[5-6], and heavy metal ion adsorption[7-9]. The application research of biochar materials in building materials not only maintains the original mechanical properties of the materials, but also introduces functions such as environmental purification and carbon dioxide sequestration[10-12]. In fact, agricultural and forestry practices are the main contributors to the large amount of biomass waste generated. Globally, approximately 140 Gt of waste is generated annually, posing a significant challenge to management as discarded biomass has a negative impact on the environment [13]. In recent years, several studies have reported the positive effects of incorporating different biochar contents and types into cementitious matrices, including improved cement hydration, contaminant fixation, fracture energy and high-temperature resistance, as well as direct and indirect effects on mechanical strength [14]. Experimental studies conducted by Gupt et al. showed that biochar particle size significantly affects the workability, hydration and mechanical properties of cementitious matrices [15]. The following year, the team further improved the strength of cement mortar under sulfate conditions by adding rice husk biochar [16]. However, these studies required the addition of silica fume to enhance concrete performance, which could potentially increase costs further. Studies by Sirico et al. showed that by adding an appropriate proportion of biochar, compressive strength and flexural strength comparable to the original material could be obtained [17]. Although biochar materials can positively impact cement properties and impart unique characteristics to cement, previous studies have not systematically investigated the mechanisms by which biochar materials affect cement hydration reactions.

In this work, two biochar materials, rice husk biochar (RB) and corn stalk biochar (CB), were mixed with conventional commercial cement to prepare cement-based composite materials (RBMC and CBMC, respectively). This study investigated the mechanical properties and hydration mechanism of cement-based composites under standard curing conditions for 28 days. Simultaneous thermal analysis (TG-DTG), X-ray diffraction (XRD), mercury intrusion porosimetry (MIP), scanning electron microscopy-energy dispersive spectroscopy (SEM-EDS), and attenuated total reflectance Fourier transform infrared spectroscopy (ATR-FTIR) were employed to study the compressive strength, flexural strength, and total calcium hydroxide generated during hydration of the cement-based composites. This research presents a valuable new development strategy for improving the performance of cement-based materials using low-cost biochar materials prepared from agricultural and forestry waste.

2. Experiments

2.1. Raw Materials and Analysis

PII 52.5 cement (PC) was used with a loss on ignition of 2.3%. The basic performance indicators and chemical composition of the cement are shown in **Table 1** and **Table 2** respectively. **Figure 1(a)** presents the particle size distribution diagram of the cement. Its particle size ranges from 2.121 **μm** to 176 **μm**, with an average particle size of 21.19 **μm**. Other materials include standard sand and tap water. The materials used in this experiment are all sponsored by Weihai Zhongheng Pipe Pile Co., Ltd.

Rice husk charcoal (RB) and corn straw charcoal (CB) were obtained through carbonization experiments. The heating rate of the muffle furnace was 5□/min, the nitrogen flow rate was 200 mL/min, and the final carbonization temperature was 500□. Before starting the heating of the muffle furnace, nitrogen was filled to expel air and form a nitrogen environment. After heating up to the final carbonization temperature, it was continuously maintained for 2 hours, and then it was automatically cooled to room temperature to obtain

[1] College of Mechanical and Electronic Engineering, Shandong Agriculture and Engineering University, Jinan 250100, China
[2] Weihai Zhongheng Pipe Pile Co., Ltd, Weihai 264200, China
[*] Corresponding Author: songyw528@163.com

Table 1. Basic performance index of cement.

Compressive strength (Mpa)		Flexural strength (Mpa)		Setting time (min)	
3d	28d	3d	28d	Initial setting	Final setting
30.8	60.1	6.9	9.5	174	225

Table 2. Chemical composition of Ordinary Portland Cement(wt%).

Oxide	CaO	SiO_2	Al_2O_3	SO_3	Fe_2O_3	MgO	Na_2O	K_2O
PC	63.57	22.84	4.91	2.69	3.46	2.73	0.18	0.64
Oxide	CaO	SiO_2	Al_2O_3	SO_3	Fe_2O_3	MgO	Na_2O	K_2O

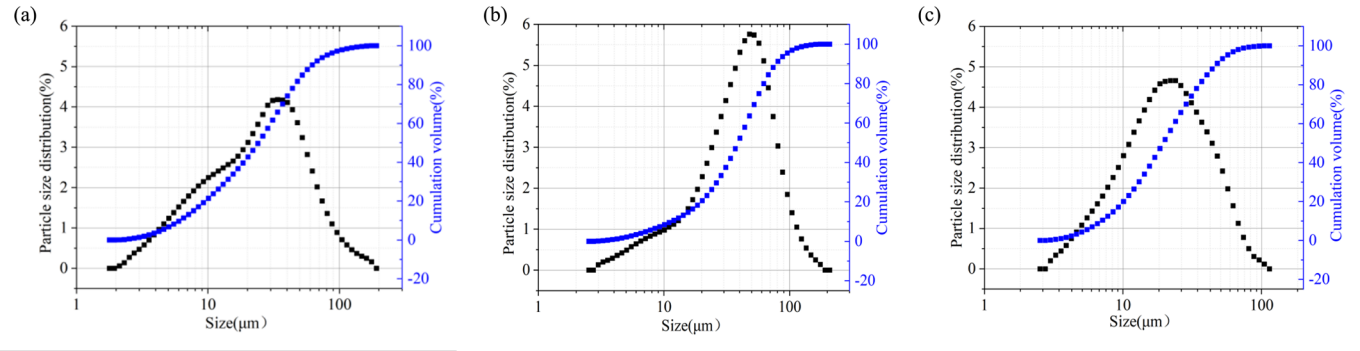

Figure 1. Particle size distribution of PC(a), RB(b) and CB(c) powder.

Table 3. Chemical element composition of RB, CB (wt%)

Sample	C	O	Si	Ca	K	Al	P	Mg	N	Fe
RB	35.33	37.91	22.78	0.52	2.54	0.03	0.24	0.16	0.00	0.07
CB	52.55	23.66	9.33	2.43	3.21	1.93	0.39	1.31	1.55	1.78

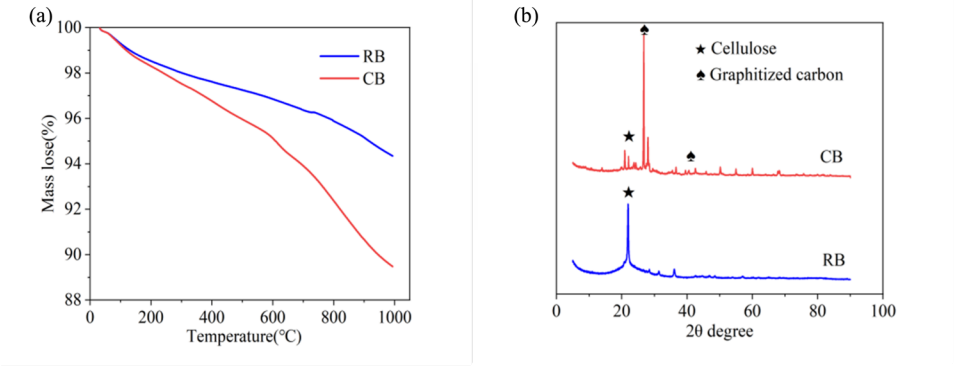

Figure 2. (a) TG result of RB and CB powder. (b)XRD pattern of RB and CB powder.

Table 4. Brunauer-Emmett-Teller (BET) surface area analysis results

Sample	BET Surface Area (m^2/g)	Total Pore Volume (cm^3/g)	Average Pore Radius (nm)
PC	1.98	0.006	12.59
RB	108.94	0.065	2.39
CB	109.97	0.059	2.16

biochar.

The chemical element compositions of RB and CB are shown in **Table 3**. The silicon element content in rice husk charcoal is relatively high. The particle size distribution diagrams of RB and CB are shown in **Figure 1(b)** and **1(c)**. The particle size range of RB is 2.999μm - 176μm, and the average particle size is 38.91μm. The particle size range of CB is 2.999μm - 104.7μm, and the average particle size is 19.49μm.

The thermogravimetric analysis results of RB and CB are shown in **Figure 2(a)**. Compared with the weight loss of approximately 5.5% for RB, CB exhibited a relatively large weight loss of 10.5%. The X-ray diffraction (XRD) analysis of RB and CB (**Figure 2(b)**) shows that both RB and CB exhibit a characteristic peak attributed to cellulose at 2θ = 22° (the peak at 2θ = 22° may also be the characteristic peak of SiO□, overlapping with that of cellulose) [18], indicating that the high - temperature preparation environment did not damage the cellulose structure of the biochar. CB shows a relatively prominent and a weak crystal diffraction peak at around 2θ = 24° and 43° respectively, indicating that CB has graphite - like microcrystalline structures to varying degrees[19].

The Brunauer-Emmett-Teller (BET) surface area, average pore diameter, and total pore volume of the three raw materials, PC, RB, and CB were tested using a fully automatic specific surface area and pore size analyzer. The results are shown in **Table 4**. The specific surface areas of RB and CB are 108.94 and 109.97 respectively, which are much higher than that of PC. It can be seen that biochar has a well - developed specific surface area. Therefore, it can be hypothesized that in the initial stage of composite material preparation, due to its well - developed specific surface area, biochar absorbs water to saturation

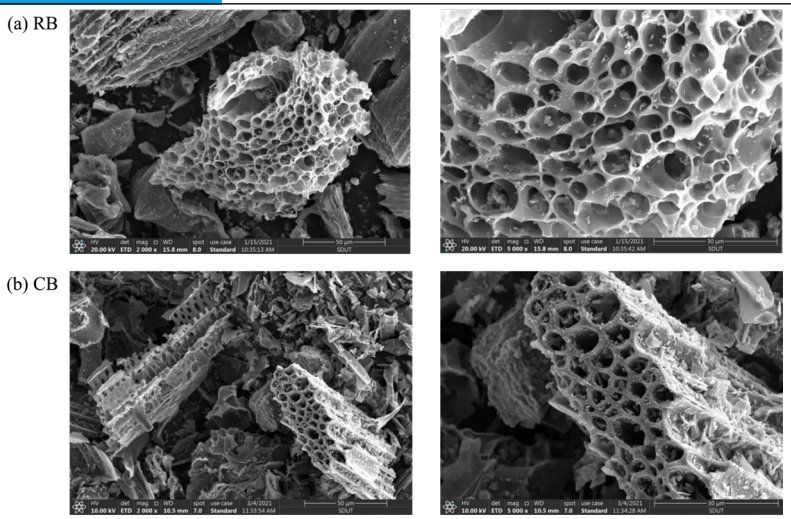

Figure 3. Morphology of RB (a) and CB (b) powder

first. As the curing progresses, the water in the biochar gradually migrates into the cement material, filling the pores of the cement - based material with non - chemically - bound water. This increases the relative humidity of the cement - based material, thus improving the curing effect of the composite material and enhancing the mechanical properties of the sample.

The micro - surface morphologies of RB and CB are shown in **Figure 3**. The surface of RB exhibits honeycomb - like macropores, while the surface of CB shows fibrous macropores. These pores may be generated during the pyrolysis process or originate from the capillary structure of the biomass raw materials. The abundant pores have strong water absorption capacity, which can thus change the water - cement ratio, consistent with the hypothesis in the BET analysis.

Table 5. Mix proportion for prepared cement mortar(g)

Samples	Water	Sand	Cement	BB biochar	w/b
Control	225	1350	450	0	0.5
RB2%	225	1350	441	9	0.5
RB4%	225	1350	432	18	0.5
RB6%	225	1350	423	27	0.5
CB2%	225	1350	441	9	0.5
CB4%	225	1350	432	18	0.5
CB6%	225	1350	423	27	0.5

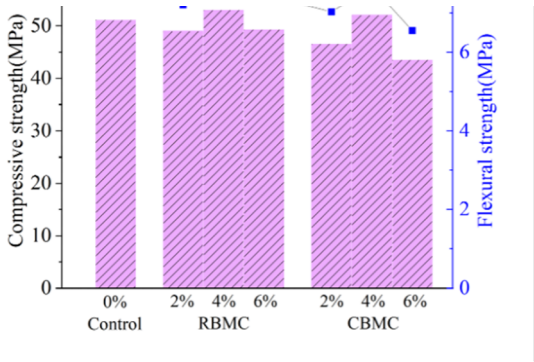

Figure 4. Compressive strength and flexural strength

2.2. Samp le Preparation and Testing Methods

The mix ratio design for the composite material is shown in **Table 5**. Referring to GB/T 17671–1999 (the current cement mortar standard of the People's Republic of China, which is not much different from standards used in other countries), the composite material is prepared into cement mortar specimens measuring 40 mm × 40 mm × 160 mm. Specimens mixed with CB and RB are abbreviated as CBMC and RBMC, respectively, with biochar materials added at 2%, 4%, and 6%. After the samples were molded in the mold for 1 day, the mold was removed, and the samples were placed in a curing room (temperature: 20 □ ± 2 □, humidity > 95%). They were cured for 28 days and then taken out for later use. The compressive strength and flexural strength of 7 groups of samples were tested respectively. Meanwhile, thermogravimetric - derivative thermogravimetric (TG - DTG) analysis and X - ray diffraction (XRD) were used to analyze the content and phase composition of the hydration products of the samples. The mercury intrusion porosimetry (MIP) was adopted to analyze the influence of the addition of biochar on the pore structure of the mortar. Fourier - transform infrared spectroscopy (FTIR) analysis was used to analyze the changes of the surface functional groups of the samples. The micro - morphology and element distribution of the samples were observed by scanning electron microscope (SEM) and energy - dispersive spectrometer (EDS).

3 Results and Discussion

The compressive strength and flexural strength values of the 7 groups of samples after 28d curing under standard conditions are shown in **Figure 4**. It can be seen from the figure that when the biochar addition amount is 4%, the strengths of RBMC and CBMC are slightly higher than those of the control group. This may be because the biochar material has a porous carbon skeleton structure with very stable properties. Its abundant micropores can store a large amount of water, which is slowly released during the hydration reaction

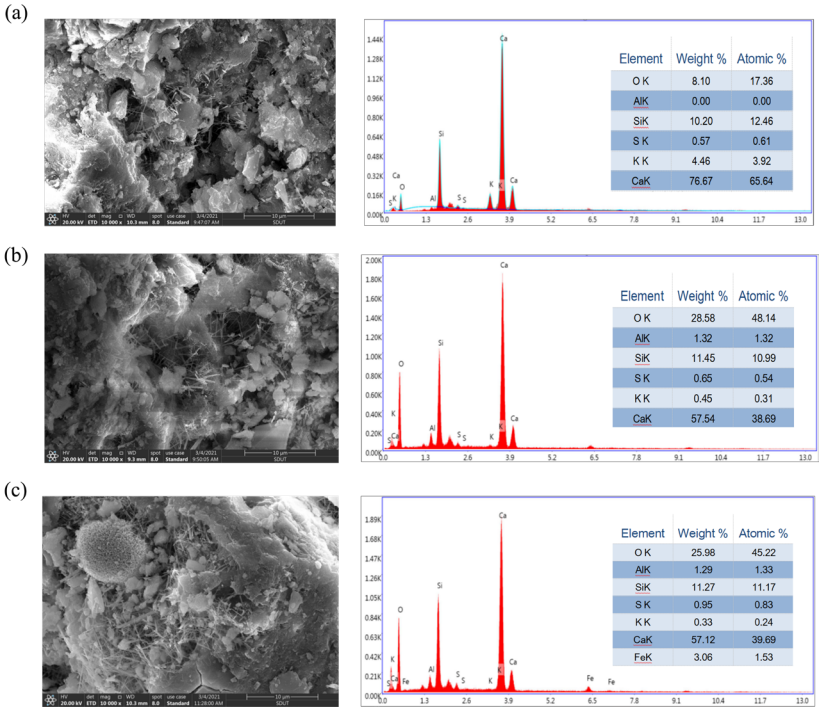

Figure 5. SEM images and EDS results of control (a), RB4% (b) and CB4% (c)

of the cement material, thus improving the degree of cement hydration and promoting the formation of hydration products (C-S-H gel)[14, 20].

At the same time, due to the filling effect of biochar, the pore size of the cement - based material can be reduced, making the composite material denser than the control group. Therefore, this experiment shows that adding a small amount of biochar can improve the mechanical properties of the cement-based material by deepening the degree of cement hydration.

However, there is a certain reasonable range for the improvement of the strength of cement specimens by biochar. When the addition amounts of RB and CB are 6%, the strengths are lower than those of the control group. The main reason is that the strength of the cement-based material comes from the products generated by the cement hydration reaction. If a large amount of cement is replaced by biochar, it will inevitably lead to a reduction in hydration products, thus reducing the mechanical properties of the cement - based material.

Therefore, this experiment can basically confirm that when the dosages of RB and CB are 4%, it has a promoting effect on the strength of cement mortar samples. In the following, the control group, RB4% and CB4% are taken as the research objects respectively to explore the influence of biochar on the cement hydration reaction.

Figure 5 shows the micro - morphology images and EDS spectra of the specimens in the blank group, RB4% and CB4% after 28 - day standard curing. From the micro - morphology images, it can be seen that the hydration products of the specimens in the blank group, RB4% and CB4% are mainly fibrous C - S - H gel and flaky calcium hydroxide. Through the analysis of the EDS spectra, the Ca/Si molar ratios of the hydration products of the three groups of specimens are 5.26, 3.52 and 3.55 respectively. Previous studies have shown that a lower Ca/Si molar ratio has a stronger adsorption capacity for alkalis. Therefore, specimens with a lower Ca/Si molar ratio can better inhibit the occurrence of the alkali - aggregate reaction (AAR). Thus, adding an appropriate amount of biochar to cement has important guiding significance for the study of concrete durability[21].

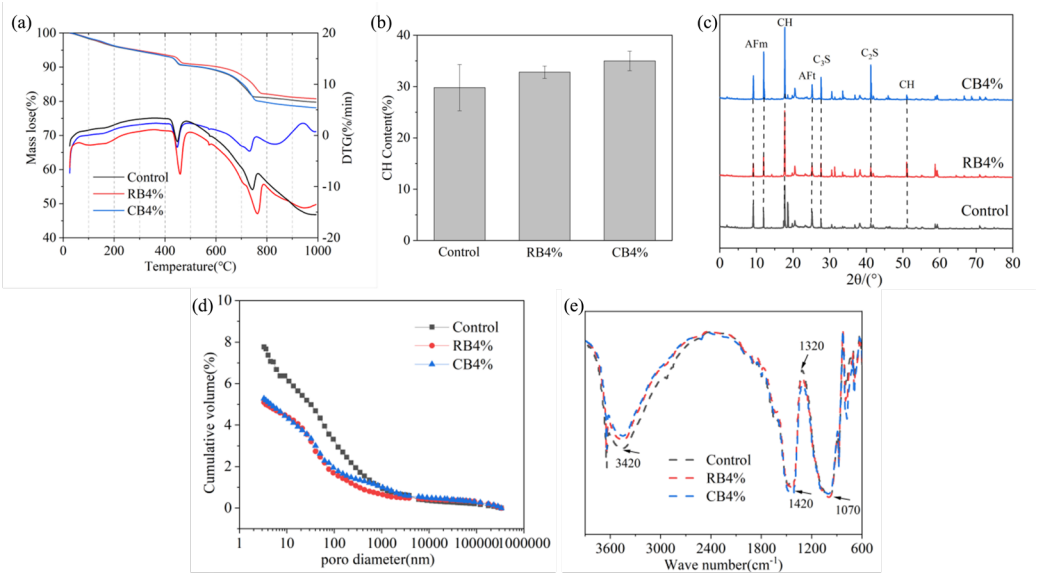

Figure 6. (a) TG/DTG curves of control, RB4% and CB4%; (b) CH content of control, RB4% and CB4%; (c) XRD patterns of control, RB4% and CB4%; (d) Cumulative distribution curves of control, RB4% and CB4%; (e) ATR-FT-IR spectras of control, RB4% and CB4%.

Figure 6(a) shows the comprehensive thermal analysis curves of the control group, RB4% and CB4% with a hydration age of 28 days. Through observation, the cement-based material has three obvious concave peaks or weight-loss segments, which are the endothermic peak of free water at 100□ - 200□, the endothermic peak of calcium hydroxide at 400□ - 470□ and the endothermic peak of calcium carbonate at 650□ - 950□. Compared with the control group, the addition of biochar led to an increasing trend in the weight loss of the cement mortar samples.

By analyzing the DTG curve of the cement - based material, it is considered that the weight loss caused by the evaporation of free water in the sample occurs when the temperature is in the range of 110□ - 400□, which is called gel weight loss. When the temperature is in the range of 400□ - 500□, the mass loss is caused by the decomposition of $Ca(OH)_2$.

Since the water generated by the decomposition of $Ca(OH)_2$ is released as water vapor, the weight loss in the DTG curve at 400□ - 500□ is the mass of water vapor. Therefore, the content of $Ca(OH)_2$ (CH, %) can be calculated.

$$CH = \frac{M_2 \times m}{M_1} \quad (1)$$

where: M_1 and M_2 are the molecular weights of H_2O and $Ca(OH)_2$ respectively, and m is the percentage of weight loss of the sample at 400□ - 500□. The analysis diagram of the content of hydration products (calcium hydroxide) of the three groups of samples is shown in **Figure 6(b)**. It can be seen from the figure that the addition of biochar does not affect the total amount of calcium hydroxide produced during the hydration process of the cement - based material.

Therefore, it can be concluded that the mechanical properties of the biochar - cement - based composite mainly come from the bridging effect of biochar at the micro - cracks in the cement - based material[22]. Biochar does not have a significant impact on the entire process of cement hydration. In addition, biochar plays a role in changing the hydration rate in the cement - based material, without changing the total amount of calcium hydroxide during the hydration reaction[23].

Figure 6(c) shows the XRD analysis patterns of the blank group, RB4% and CB4%. In the figure, when the angle is 18°, it corresponds to the CH diffraction peak. By comparing the two experimental groups with the blank group, it is found that the diffraction peak values are basically the same. This indicates that the incorporation of biochar does not generate new hydration products, but changes the diffraction peak values of the existing hydration products. That is to say, the incorporation of biochar affects the morphology and quantity of the existing hydration products. This is consistent with the results of the thermogravimetric analysis.

Compared with the blank group, the conversion degree of C_3S and C_2S into calcium hydroxide in the two experimental groups is higher, indicating that the addition of biochar can promote the hydration reaction process of the cement - based material, thus obtaining higher mechanical properties. From the above experimental results, it can be concluded that adding biochar to the cement - based material does not change the total amount of calcium hydroxide generated during the hydration process of the cement - based material, but only affects the crystalline form of calcium hydroxide, which is roughly consistent with the view of Kowald[23].

Figure 6(d) shows the cumulative pore size distribution curves of the control group, RB4% and CB4% samples after 28 - day curing. As can be seen from the figure, the porosities of the control group, RB4% and CB4% samples are 7.9%, 5.1% and 5.3% respectively. Due to the addition of biochar, compared with the control group, the porosities of the samples decreased by 35.4% and 32.9% respectively. It can be seen that the pore size of the cement mortar has been refined, with a reduction in large pores and an increase in small pores, making the samples denser. This verifies the hypothesis when analyzing the results of the mechanical experiments.

Figure 6(e) shows the infrared spectral curves of the control group, RB4% and CB4% samples after 28 - day curing. The three curves basically overlap completely, indicating that there is no significant difference in the hydration products between the two experimental groups and the control group. There is a distinct absorption peak at 1070 cm□¹, corresponding to the Si - O stretching vibration[24]. There is also an absorption peak at 1420 cm□¹, corresponding to the C - O symmetric stretching vibration. Therefore, the formation of C - S - H gel can be inferred[25]. In addition, the vibration band at 3420 cm□¹ corresponds to the H - OH group, and the absorption peak at 1320 cm□¹ corresponds to the asymmetric stretching mode of the CO□²□ group[24]. From the obtained results, it can be speculated that the strength of the samples may come from the formation of calcium silicate hydrate (C - S - H) gel. In addition, the RB4% experimental group produced the highest C - S - H band, indicating that during the development of cement hydration, RB is more likely to integrate into the cement - based material than CB.

4. Conclusions

This study used two types of biochar (RB and CB) as raw materials to replace cement in the preparation of cement mortar samples at dosages of 2%, 4%, and 6%, respectively. The mechanical properties and hydration mechanisms of the samples after 28 days of standard curing were investigated. Mechanical property tests showed that when the biochar (RB, CB) dosage was 4%, the compressive and flexural strengths of RBMC and CBMC were higher than those of the control group. This indicates that there is an optimal value for the biochar dosage; too high or too low a dosage is not optimal. SEM images showed that the cement hydration products of all three samples were fibrous C-S-H gel and lamellar CH. EDS spectroscopy showed that the Ca/Si molar ratio of the C-S-H gel in RBMC and CBMC was lower than that in the control group. TG-DTG, XRD, and ATR-FTIR experiments indicated that adding biochar to cement-based materials did not change the types of hydration products or the total amount of calcium hydroxide formed. In the infrared spectrum, a distinct absorption peak was observed at 1070 cm□¹, corresponding to the stretching vibration of Si-O, thus confirming the presence of C-S-H. Furthermore, the C-S-H absorption peak intensity was highest in the RB 4% experimental group, indicating that RB is more readily incorporated into cement-based materials than CB during cement hydration. MIP experimental results further confirmed that biochar can refine the pore size of cement mortar. Adding an appropriate amount of biochar can reduce the macropore size and increase the micropore size of cement paste, making the mortar denser and stronger. This work demonstrates the significant role of biochar in the durability of cement-based materials.

5. Future work

This research shows that it is beneficial to add biochar materials to cement. Next, our research group will focus on exploring the role of biochar in foam concrete materials.

CRediT authorship contribution statement

Ning Song: Conceptualization, Methodology, Validation, Formal analysis, Data curation, Investigation, Writing-original draft; Guangqi Hu: Formal analysis, Data curation.

Declaration of competing interest

The authors declare that they have no known competing financial interests or personal relationships that could have appeared to influence the work reported in this paper.

Data availability

The data that has been used is confidential.

Acknowledgments

This work was supported by Shandong Agriculture and Engineering University Start-Up Fund for Talented Scholars (2025GCCZR-02).

References

[1] Q. Hu, J. Jung, D. Chen, K. Leong, S. Song, F. Li, B. C. Mohan, Z. Yao, A. K. Prabhakar, X. H. Lin, E. Y. Lim, L. Zhang, G. Souradeep, Y. S. Ok, H. W. Kua, S. F. Y. Li, H. T. W. Tan, Y. Dai, Y. W. Tong, Y. Peng, S. Joseph, C.-H. Wang. "Biochar industry to circular economy." *Sci. Total Environ.* **2021**, *757*, 143820.

[2] K. Y. Chan, L. Van Zwieten, I. Meszaros, A. Downie, S. Joseph. "Agronomic values of greenwaste biochar as a soil amendment." *Soil Res.* **2007**, *45*, 8, 629–34.

[3] A. González-Cencerrado, J. P. Ranz, M. T. López-Franco Jiménez, B. R. Gajardo. "Assessing the environmental benefit of a new fertilizer based on activated biochar applied to cereal crops." *Sci. Total Environ.* **2020**, *711*, 134668.

[4] K. cheng Shan, Q. hong Feng, X. wei Li, X. ong Meng, H. kuan Lyu, C. feng Wang, L. yang Mu, X. Liu. "C3-light lightweight algorithm optimization under YOLOv5 framework for apple-picking recognition." *X-discip.* **2025**, *1*, 1.

[5] Z. Zhang, H. Wang, J. shuo Li, H. Fu. "Recent applications of metal additive manufacturing: a review." *X-discip.* **2025**, *1*, 1.

[6] N. Priyadarshni, P. Nath, Nagahanumaiah, N. Chanda. "Sustainable removal of arsenate, arsenite and bacterial contamination from water using biochar stabilized iron and copper oxide nanoparticles and associated

mechanism of the remediation process." *J. Water Process Eng.* **2020**, *37*, 101495.
[7] J. Li, Y. Li, Y. Wu, M. Zheng. "A comparison of biochars from lignin, cellulose and wood as the sorbent to an aromatic pollutant." *J. Hazard. Mater.* **2014**, *280*, 450–57.
[8] L. Wang, L. Chen, D. C. W. Tsang, H. W. Kua, J. Yang, Y. S. Ok, S. Ding, D. Hou, C. S. Poon. "The roles of biochar as green admixture for sediment-based construction products." *Cem. Concr. Compos.* **2019**, *104*, 103348.
[9] P. Maneechakr, S. Mongkollertlop. "Investigation on adsorption behaviors of heavy metal ions (Cd2+, Cr3+, Hg2+ and Pb2+) through low-cost/active manganese dioxide-modified magnetic biochar derived from palm kernel cake residue." *J. Environ. Chem. Eng.* **2020**, *8*, 6, 104467.
[10] Y. Qin, X. Pang, K. Tan, T. Bao. "Evaluation of pervious concrete performance with pulverized biochar as cement replacement." *Cem. Concr. Compos.* **2021**, *119*, 104022.
[11] C. Xie, L. Yuan, H. Tan, Y. Zhang, M. Zhao, Y. Jia. "Experimental study on the water purification performance of biochar-modified pervious concrete." *Constr. Build. Mater.* **2021**, *285*, 122767.
[12] A. Osman, S. Fawzy, M. Farghali, M. El-Azazy, A. Elgarahy, R. Fahim, M. Maksoud, A. Ajlan, M. Yousry, Y. Saleem, D. Rooney. "Biochar for agronomy, animal farming, anaerobic digestion, composting, water treatment, soil remediation, construction, energy storage, and carbon sequestration: a review." *Environ. Chem. Lett.* **2022**, *20*, 4, 2385–485.
[13] N. P. F. Coelho, G. H. Nalon, J. F. Mendes, T. J. P. de Oliveira, R. F. Mendes. "Effects of coffee husk biochar on the properties of concrete." *Constr. Build. Mater.* **2025**, *491*, 142680.
[14] Gupta Souradeep, Kua Harn Wei. "Factors determining the potential of biochar As a carbon capturing and sequestering construction material: critical review." *J. Mater. Civ. Eng.* **2017**, *29*, 9, 4017086.
[15] S. Gupta, P. Krishnan, A. Kashani, H. W. Kua. "Application of biochar from coconut and wood waste to reduce shrinkage and improve physical properties of silica fume-cement mortar." *Constr. Build. Mater.* **2020**, *262*, 120688.
[16] S. Gupta, S. Muthukrishnan, H. W. Kua. "Comparing influence of inert biochar and silica rich biochar on cement mortar – hydration kinetics and durability under chloride and sulfate environment." *Constr. Build. Mater.* **2021**, *268*, 121142.
[17] A. Sirico, P. Bernardi, B. Belletti, A. Malcevschi, E. Dalcanale, I. Domenichelli, P. Fornoni, E. Moretti. "Mechanical characterization of cement-based materials containing biochar from gasification." *Constr. Build. Mater.* **2020**, *246*, 118490.
[18] R. Amen, M. Yaseen, A. Mukhtar, J. J. Klemeš, S. Saqib, S. Ullah, A. G. Al-Sehemi, S. Rafiq, M. Babar, C. L. Fatt, M. Ibrahim, S. Asif, K. S. Qureshi, M. M. Akbar, A. Bokhari. "Lead and cadmium removal from wastewater using eco-friendly biochar adsorbent derived from rice husk, wheat straw, and corncob." *Cleaner Eng. Technol.* **2020**, *1*, 100006.
[19] L. Sui, C. Tang, Q. Du, Y. Zhao, K. Cheng, F. Yang. "Preparation and characterization of boron-doped corn straw biochar: Fe (□) removal equilibrium and kinetics." *J. Environ. Sci.* **2021**, *106*, 116–23.
[20] L. Chen, Y. Zhang, L. Wang, S. Ruan, J. Chen, H. Li, J. Yang, V. Mechtcherine, D. Tsang. "Biochar-augmented carbon-negative concrete." *Chem. Eng. J.* **2022**, *431*.
[21] B. Li, S. Wang, D. Pan, Y. Zhang. "Hydration Products and Mechanical Properties of Steam Cured Lithium Slag Blended Cement." *J. Chin. Ceram. Soc.* **2019**, 7, 891–99.
[22] J. M. Makar, G. W. Chan. "Growth of cement hydration products on single□walled carbon nanotubes." *J. Am. Ceram. Soc.* **2009**, *92*, 6, 1303–10.
[23] T. Kowald, R. Trettin. "Improvement of cementitious binders by multi-walled carbon nanotubes." **2009**, 261–66.
[24] I. Ismail, S. A. Bernal, J. L. Provis, R. San Nicolas, S. Hamdan, J. S. J. Van Deventer. "Modification of phase evolution in alkali-activated blast furnace slag by the incorporation of fly ash." *Cem. Concr. Compos.* **2014**, *45*, 125–35.
[25] R. Alghamri, A. Kanellopoulos, A. Al-Tabbaa. "Impregnation and encapsulation of lightweight aggregates for self-healing concrete." *Constr. Build. Mater.* **2016**, *124*, 910–21.